INTERNATIONAL JOURNAL OF
RADIATION ONCOLOGY • BIOLOGY • PHYSICS
www.redjournal.org

PHYSICS CONTRIBUTION

A Framework for Assessing the Effect of Cardiac and Respiratory Motion for Stereotactic Arrhythmia Radioablation Using a Digital Phantom With a 17-Segment Model: A STOPSTORM.eu Consortium Study

Raoul R.F. Stevens, PhD,[*] Colien Hazelaar, PhD,[*] Marta Bogowicz, PhD,[*] Rachel M.A. ter Bekke, PhD,[†] Paul G.A. Volders, PhD,[†] Karolien Verhoeven, PhD,[*] Dirk de Ruysscher, PhD,[*] Joost J.C. Verhoeff, PhD,[‡] Martin F. Fast, PhD,[‡] Stefano Mandija, PhD,[‡] Jakub Cvek, PhD,[§] Lukas Knybel, PhD,[§] Pavel Dvorak, PhD,[§] Oliver Blanck, PhD,[‖] and Wouter van Elmpt, PhD[*]

[*]*Department of Radiation Oncology (Maastro), GROW School for Oncology and Reproduction, Maastricht University Medical Center +, Maastricht, The Netherlands;* [†]*Department of Cardiology, Cardiovascular Research Institute Maastricht, Maastricht University Medical Center+, Maastricht, The Netherlands;* [‡]*Department of Radiotherapy, University Medical Center Utrecht, Utrecht, The Netherlands;* [§]*Department of Oncology, University Hospital and Faculty of Medicine, Ostrava, Czech Republic; and* [‖]*Department of Radiation Oncology, University Medical Center Schleswig-Holstein, Kiel, Germany*

Received May 10, 2023; Accepted for publication Aug 22, 2023

Purpose: The optimal motion management strategy for patients receiving stereotactic arrhythmia radioablation (STAR) for the treatment of ventricular tachycardia (VT) is not fully known. We developed a framework using a digital phantom to simulate cardiorespiratory motion in combination with different motion management strategies to gain insight into the effect of cardiorespiratory motion on STAR.

Methods and Materials: The 4-dimensional (4D) extended cardiac-torso (XCAT) phantom was expanded with the 17-segment left ventricular (LV) model, which allowed placement of STAR targets in standardized ventricular regions. Cardiac- and respiratory-binned 4D computed tomography (CT) scans were simulated for free-breathing, reduced free-breathing, respiratory-gating, and breath-hold scenarios. Respiratory motion of the heart was set to population-averaged values of patients with

Corresponding author: Raoul R. F. Stevens, PhD; E-mail: raoul.stevens@maastro.nl

This study is part of the project "Standardized Treatment and Outcome Platform for Stereotactic Therapy Of Re-entrant tachycardia by a Multidisciplinary (STOPSTORM) Consortium," which has received funding from the European Union's Horizon 2020 research and innovation program under grant agreement No. 945119.

Disclosures: D.D.R. received support and research grants (paid to the institution) from AstraZeneca, BMS (Bristol Myers Squibb), Beigene, Philips, Olink, and Eli Lilly. In addition, he was a member of the advisory boards for these companies. M.F.F. received 2 research grants from the NWO (Nederlandse Organisatie voor Wetenschappelijk Onderzoek; EN: Dutch Research Council) under grant numbers 17515 and 19484 (payment to institution) and is the lead of the AAPM/EFOMP TG-391 (American Association of Physicists in Medicine/European Federation of Organisations for Medical Physics Task Group-391) task group on 4-dimensional magnetic resonance imaging (unpaid). O.B. is a board member of the DEGRO (Deutsche Gesellschaft Für Radioonkologie e.V.) and the DGMP (Deutsche Gesellschaft für Medizinische Physik e.V.) working group SRT (Stereotactic Radiotherapy) and is the Medical Physics section editor for the *Strahlentherapie und Onkologie* journal. Furthermore, he is a board member and the work package 4 lead of the Horizon 2020 grant number 945119 (funding as specified in the agreement). Finally, J.C. received a research grant from the Ministry of Health of the Czech Republic under grant number NU20-02-00244 and received money from Accuray.

Data Sharing Statement: Research data (ie, parameter files) are available in the supplementary materials.

Supplementary material associated with this article can be found in the online version at doi:10.1016/j.ijrobp.2023.08.059.

Acknowledgments—The authors thank all members of the STOPSTORM consortium (see https://stopstorm.eu/en/consortium).

Int J Radiation Oncol Biol Phys, Vol. 118, No. 2, pp. 533–542, 2024

https://doi.org/10.1016/j.ijrobp.2023.08.059

VT: 6, 2, and 1 mm in the superior-inferior, posterior-anterior, and left-right direction, respectively. Cardiac contraction was adjusted by reducing LV ejection fraction to 35%. Target displacement was evaluated for all segments using envelopes encompassing the cardiorespiratory motion. Envelopes incorporating only the diastole plus respiratory motion were created to simulate the scenario where cardiac motion is not fully captured on 4D respiratory CT scans used for radiation therapy planning.

Results: The average volume of the 17 segments was 6 cm^3 (1-9 cm^3). Cardiac contraction-relaxation resulted in maximum segment (centroid) motion of 4, 6, and 3.5 mm in the superior-inferior, posterior-anterior, and left-right direction, respectively. Cardiac contraction-relaxation resulted in a motion envelope increase of 49% (24%-79%) compared with individual segment volumes, whereas envelopes increased by 126% (79%-167%) if respiratory motion also was considered. Envelopes incorporating only the diastole and respiration motion covered on average 68% to 75% of the motion envelope.

Conclusions: The developed LV-segmental XCAT framework showed that free-wall regions display the most cardiorespiratory displacement. Our framework supports the optimization of STAR by evaluating the effect of (cardio)respiratory motion and motion management strategies for patients with VT.

Introduction

The delivery of stereotactic radiation therapy to the arrhythmogenic substrate within the left ventricle (LV) of the heart, called stereotactic arrhythmia radioablation (STAR), is a new and promising treatment option for patients with refractory ventricular tachycardia (VT).[1-5] To deliver STAR, the arrhythmogenic substrate needs to be characterized using, for instance, invasive electro-anatomic mapping. However, delineating the identified target on the radiation therapy planning computed tomography (CT) scan is not easy as the target is mostly defined based on the electrical properties, which are not visible on the planning CT scan. The American Heart Association (AHA) 17-segment LV model,[6,7] a standardized myocardial segmentation for cardiac imaging commonly used in cardiology (Fig. 1), can be helpful to identify the target region between different modalities. Therefore, some centers base their target definition on the 17-segment segmentation,[8,9] where (parts of) one or more segments are denoted as the target volume for

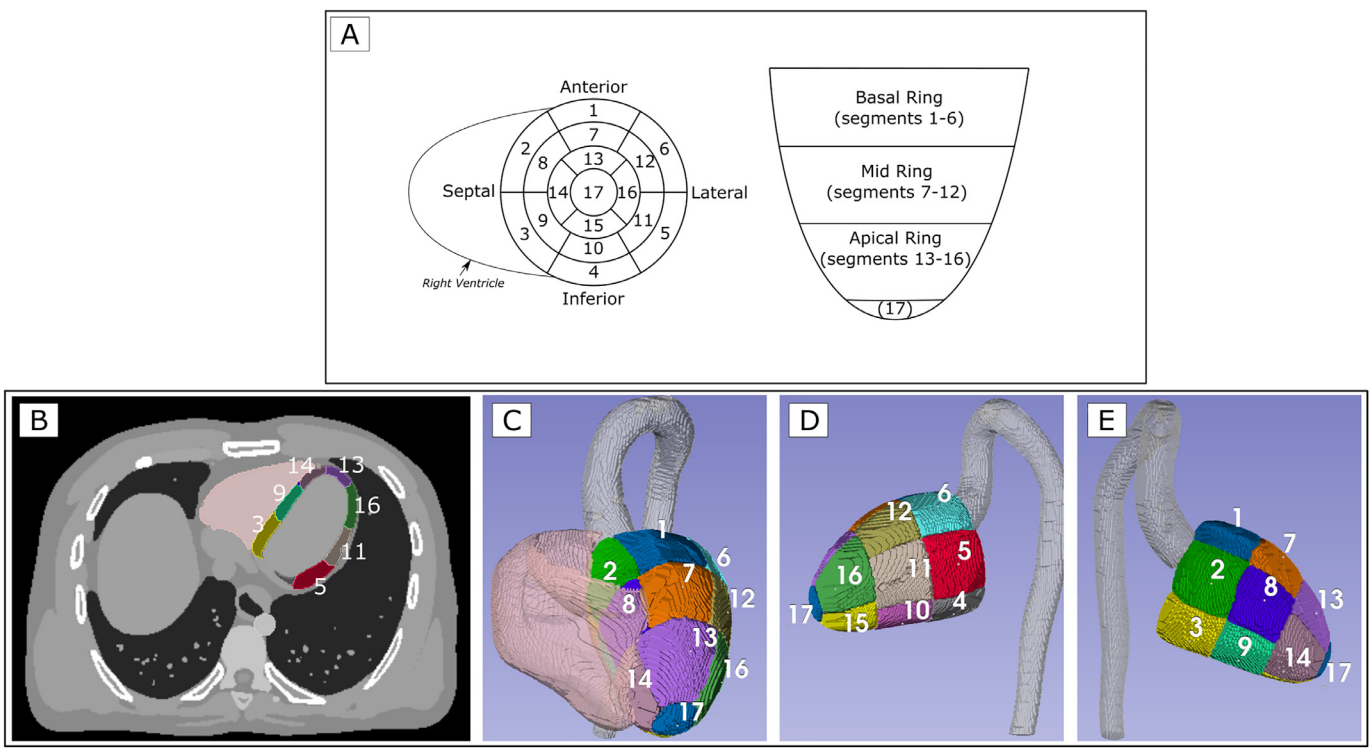

Fig. 1. (A) Overview of the 17 segments as defined in the American Heart Association 17-segment model,[6,7] with the short axis view on the left and the long axis view on the right. (B) Axial slice of the extended cardiac-torso (XCAT) phantom with the delineation of the right ventricle in pink and some of the left ventricle segments visible. (C-E) Three-dimensional view showing the parameterized left ventricular 17-segment model in the digital XCAT phantom from the anterior, lateral, and septal side of the left ventricle, respectively. In addition, the aorta is visible in gray.

STAR. However, delivering the prescribed radiation dose (typically 20-25 Gy) in a single fraction to this target can be challenging because of target motion due to breathing and cardiac contraction. We recently performed a literature review[10] that showed average motion due to cardiac contraction-relaxation ("cardiac motion") of STAR targets to be <5 mm in all directions, with maximum values of 8, 6, and 6.5 mm in the superior-inferior (SI), left-right (LR), and posterior-anterior (PA) direction, respectively. The combined cardiac and respiratory motion ("cardiorespiratory motion") resulted in average motion of 5 to 7 mm in the SI direction, whereas motion in PA and LR was comparable to cardiac motion alone. Cardiorespiratory motion can be incorporated into the treatment planning phase using various techniques, such as an internal target volume (ITV) approach based on time-resolved imaging, gating techniques, or tracking of the target or surrogate structures. However, clinicians face a difficult decision of whether to perform patient-specific assessment of cardiac motion. Cardiac-binned scans, needed to perform such analysis, can often not be performed within the radiation therapy center, and assessing cardiac motion from these scans is time-consuming. As a result, there is debate among experts on whether patient-specific cardiac motion assessment is necessary and worth the effort. Gaining more insight into the effect of cardiac (and respiratory) motion is therefore crucial. Furthermore, the effect of motion management techniques on the efficacy and safety of STAR is also not yet fully known and should be investigated further.

The Standardized Treatment and Outcome Platform for Stereotactic Therapy Of Re-entrant tachycardia by a Multidisciplinary (STOPSTORM) consortium (STOPSTORM.eu, Horizon 2020, GA No. 945119)[11] project will define quality requirements for treatment preparation and delivery, including the assessment of the effect of cardiorespiratory motion on STAR. To investigate this effect, "ground-truth" cardiac and respiratory targets and organ motion are needed. Obtaining ground-truth motion from patient data can be challenging due to, for example, the time resolution dependence of the data acquisition and measurement inaccuracies. In addition, the consistency of patient data is often affected by differences in image acquisition, image artifacts, and missing values, making a robust comparison of different scenarios challenging. Phantom studies, on the other hand, allow for a thorough evaluation because the ground-truth is known. Moreover, phantoms allow for the investigation of different treatment scenarios while other parameters are unchanged. In addition, the combination of realistic phantoms and motion conditions can be used to assess the effect of imaging artifacts on the accuracy of motion assessment.

Unfortunately, the number of physical phantoms that mimic both the anatomy and cardiorespiratory motion of patients is limited. There are, however, digital phantoms capable of imitating human anatomy and motion/deformation of patients that can be used to investigate different motion scenarios while maintaining a reliable ground-truth motion. A commonly used digital phantom is the 4-dimensional (4D) extended cardiac-torso (XCAT) phantom,[12] which can be used to simulate cardiac and respiratory motion for different organs, anatomies, and image modalities. This phantom has already been used in the context of STAR to validate cardiac tracking algorithms for both MRI-guided[13] and x-ray guided[14] treatment for atrial fibrillation.

In this study, we expand the capabilities of the XCAT phantom to assess the effect of cardiorespiratory motion on STAR for patients with VT. Therefore, we built a framework around the XCAT phantom that mimics cardiorespiratory motion in patients with VT during different motion management scenarios for different regions of the heart. The XCAT phantom was expanded with the AHA LV 17-segment model. To demonstrate the possibilities of this framework, we used the average motion values[10] to simulate cardiorespiratory motion in patients with VT and evaluate the geometric effect of this motion for various motion management scenarios.

Methods and Materials

Digital phantom: 17-segment LV model

The 4D extended cardiac-torso XCAT phantom (Segars et al[15]) was used as the starting point for the framework. This phantom allows for the creation of artificial 4D CT scans, based on user-defined cardiac and respiratory motion parameters. The original XCAT phantom was expanded with the AHA 17-segment LV model.[7] The model divides the LV into a basal, mid, and apical ring, each covering almost one-third of the LV from base to apex. Subsequently, the basal and mid rings are divided into 6 segments of 60° each, resulting in segments 1 to 6 and 7 to 12, for the basal and mid ring, respectively. The apical ring is separated into 4 segments of 45°, indicated by the numbers 13 to 16. Finally, segment 17 is placed at the true apex. The individual segments were parametrized in XCAT based on the anatomic region definitions from the 17-segment model (parameters provided in Table E1). In this study, we regarded each one of the 17 implemented segments as an individual fictive target volume for STAR. This allowed us to quantify the possible geometric effect of cardiorespiratory motion on STAR for predefined regions of the LV.

Cardiorespiratory motion simulations

The XCAT phantom was used to create multiple phases of cardiac- and respiratory-binned CT scans with a voxel size of $1 \times 1 \times 1$ mm^3. A complete overview of the parameters is provided in Table E2. For the free-breathing (fb) scenario, cardiac motion was divided into 5 phases for 10 different respiratory levels, resulting in a total of 50 3D CT scans (Fig. 2). The cardiac and respiratory cycles were set to 1 and 5 seconds, respectively. Translation of the heart due to

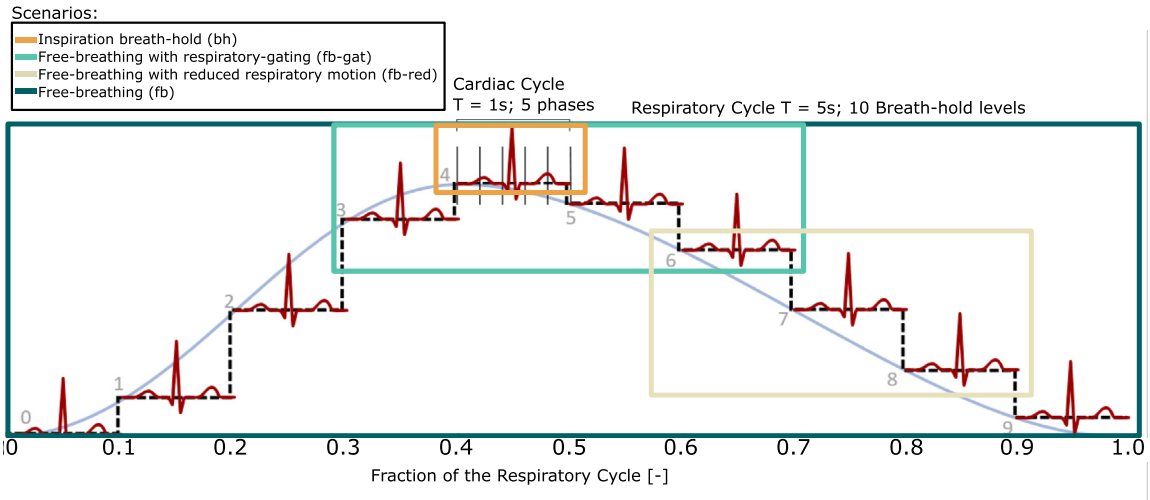

Fig. 2. Schematic overview of the respiratory levels included in the 4 different scenarios that were simulated, that is, free-breathing (fb), cardiac motion only during inspiration breath-hold (bh), free-breathing with reduced respiratory motion (fb-red), and free-breathing during respiratory-gating (fb-gat).

breathing was set to population-averaged values of patients with VT (n = 94) based on the cardiorespiratory motion of cardiac (sub)structures in our previously performed literature review,[10] that is, 6, 2, and 1 mm in the SI, PA, and LR direction, respectively. Cardiac contraction was simulated using baseline XCAT values; however, the end-systolic volume of the LV was increased to resemble an LV ejection fraction (EF) of an example patient with VT with an EF of 35%.[16] Parameter files used to set up the XCAT simulations are provided in Supplementary Materials Appendix E1. The constructed scans were then used to create 3 other scenarios (Fig. 2): (1) cardiac motion only during inspiration breath-hold (bh) consisting of the 5 CT scans with the cardiac phases at the end-inspiration respiratory level, (2) free-breathing with reduced ("shallow breathing") respiratory motion (fb-red) containing 15 CT scans, that is, the 3 respiratory levels that are centered around the mid-breathing position of the full free-breathing scenario (ie, respiratory level 7) with 5 cardiac phases each, and (3) cardiorespiratory free-breathing during gating (fb-gat) that contained 25% of the total breathing amplitude in the SI direction (20 CT scans, ie, 4 respiratory levels with 5 cardiac phases each). Inspiration breath-hold was chosen because it has the potential to reduce the dose to the organs at risk in a clinical treatment scenario.[17] The respiratory-gating window for the fb-gat scenario was chosen around full inspiration to make the comparison between limited respiratory motion versus cardiac motion only (ie, bh scenario), easier. However, in a clinical scenario also expiration breath-hold and an expiration gating window are valid options.

Analysis of motion

The 3D target volumes (ie, the 17 individual segments), the LV, and the heart were extracted from all 3D CT scans for each of the different scenarios and used to assess cardiac and/or respiratory motion amplitudes for each segment and the LV. The organ labels output of the XCAT phantom were used to automatically segment these structures of interest. Subsequently, the centroids were calculated for each of the structures of interest and the centroid motion was tracked in the SI, LR, and PA directions.

ITV definition

Besides the absolute displacement of the segments measured by the centroids, also the geometric effect of cardiac and cardiorespiratory motion on the target volume was evaluated. For this, the 3D target volumes, segmented on each of the 3D CT scans, were used to construct envelopes (E) that encompass the complete cardiac and/or respiratory motion for each of the 17 targets for the motion scenarios mentioned previously (ie, E_{bh}, $E_{fb\text{-}gat}$, $E_{fb\text{-}red}$, E_{fb}). To investigate the scenario when cardiac motion is not included in the motion envelopes, we constructed envelopes that only included the target positions in the diastolic cardiac phases during all respiratory scans associated with scenario x (E_{x_dia}).

Finally, we assessed whether a margin of 3 mm placed around E_{x_dia}, could be used to cover cardiac contraction. This margin was chosen because it is often used to account for cardiac motion during treatment with respiratory tracking.[18,19] An additional set of envelopes was created by expanding all envelopes that only included the diastolic cardiac phase(s) with an isotropic margin of 3 mm. An overview of the motion envelope construction is depicted in Figure 3.

Analysis of volumes

Volumes and increases in volume with respect to the original target volumes were calculated for each of the envelope

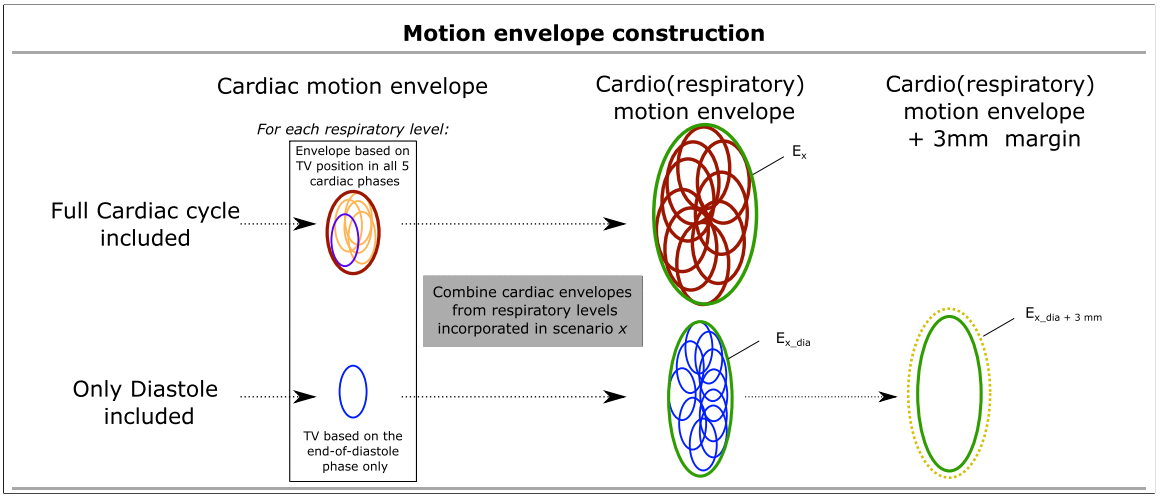

Fig. 3. Schematic depiction of the construction of the motion envelopes (E). The cardiac phases, that is, the full cardiac cycle (orange) and the end-diastolic phase (blue), are identified for each of the respiratory levels and combined in a cardiac motion envelope (red). Subsequently, the cardiac envelopes for the respiratory levels included in each of the 4 simulated scenarios, that is, breath-hold, respiratory-gating, reduced free-breathing, and free-breathing, are combined in the cardio(respiratory) envelope (green), resulting in either E_x or E_{x_dia}, where the latter was also extended with a 3 mm margin to form $E_{x\_dia\ +\ 3\ mm}$ (yellow dotted line). *Abbreviation*: TV = target volume.

definitions described previously (ie, E_x, E_{x_dia}, and $E_{x\_dia\ +\ 3\ mm}$), for each of the 4 scenarios (x) and for each segment separately. In addition, also the geometric coverage and geometric spillage were calculated to evaluate these envelopes. Here, coverage refers to the percentage of the envelope constructed based on all cardiac phases (E_x) that is covered by the motion envelope that was constructed using only the diastolic cardiac phases (E_{x_dia}). This quantifies the amount of full motion envelope that is covered when only the diastolic cardiac phase is taken into account. Spillage (%) refers to the amount of $E_{x\_dia\ +\ 3\ mm}$ that lies outside of E_x, which quantifies the amount of overcontouring compared with the full motion envelope, which clinically would lead to an increased dose to healthy tissue.

Results

Motion amplitudes

Setting the EF to 35% resulted in absolute maximum cardiac motion (bh) of the LV (center of mass) of 1.3 mm in the SI, 3.4 mm in the PA, and 1.1 mm in the LR direction. Cardiorespiratory motion of the LV was 7.3 mm in the SI, 5.4 mm in the PA, and 2.1 mm in the LR direction in the full free-breathing simulation (fb). The cardiorespiratory motion decreased to 5.3 (SI), 4.9 (PA), and 1.6 (LR) mm in the reduced free-breathing simulation (fb-red) and to 2.8 (SI), 3.9 (PA), and 1.4 (LR) mm in the simulation that mimics a respiratory-gating (fb-gat) approach. Figure 4 shows the cardiac and cardiorespiratory motion in the 3 principal directions and the 3D vector for each of the individual segments. Motion is different for each of the segments where segments near the free wall of the LV, that is, 4, 5, 6, and 10, 11, 12, and 15 and 16, can move up to 2 times more than segments located on the corresponding septal side.

Effect of motion on the target volumes

The volumes of the 17 segments and the envelopes for the 4 different scenarios are shown in Figure 5. Segment volumes in the diastolic phase during full inspiration breath-hold were on average 6 cm^3 (1-9 cm^3). Cardiac motion resulted in a cardiac envelope volume (E_{bh}) of on average 9.1 cm^3 (2-16 cm^3), which was 149% (124%-179%) of the original target volumes. The combination of cardiac and respiratory motion resulted in an envelope volume (E_{fb}) of on average 14 cm^3 (3-21 cm^3), which was 226% (179%-267%) of the initial target volumes, whereas the reduced free-breathing scenario resulted in an average envelope volume ($E_{fb\text{-}red}$) of 11 cm^3 (2-18 cm^3), which was 187% (155%-223%) of the original target volumes. The respiratory-gating approach resulted in an average envelope volume ($E_{fb\text{-}gat}$) of 10 cm^3 (2-17 cm^3), which was 169% (143%-201%) of the original target volumes. Furthermore, motion envelope volumes were largest for the basal segments located at the free wall of the LV after the larger motion of these segments.

Coverage and spillage

Average volumes and geometric coverage and spillage for the envelopes that were constructed using only the diastolic cardiac phase (in combination with corresponding respiratory phases) are shown in Table 1. An overview per target location can be found in the supplementary materials (Figs. E1-E4). Coverage increased with increasing

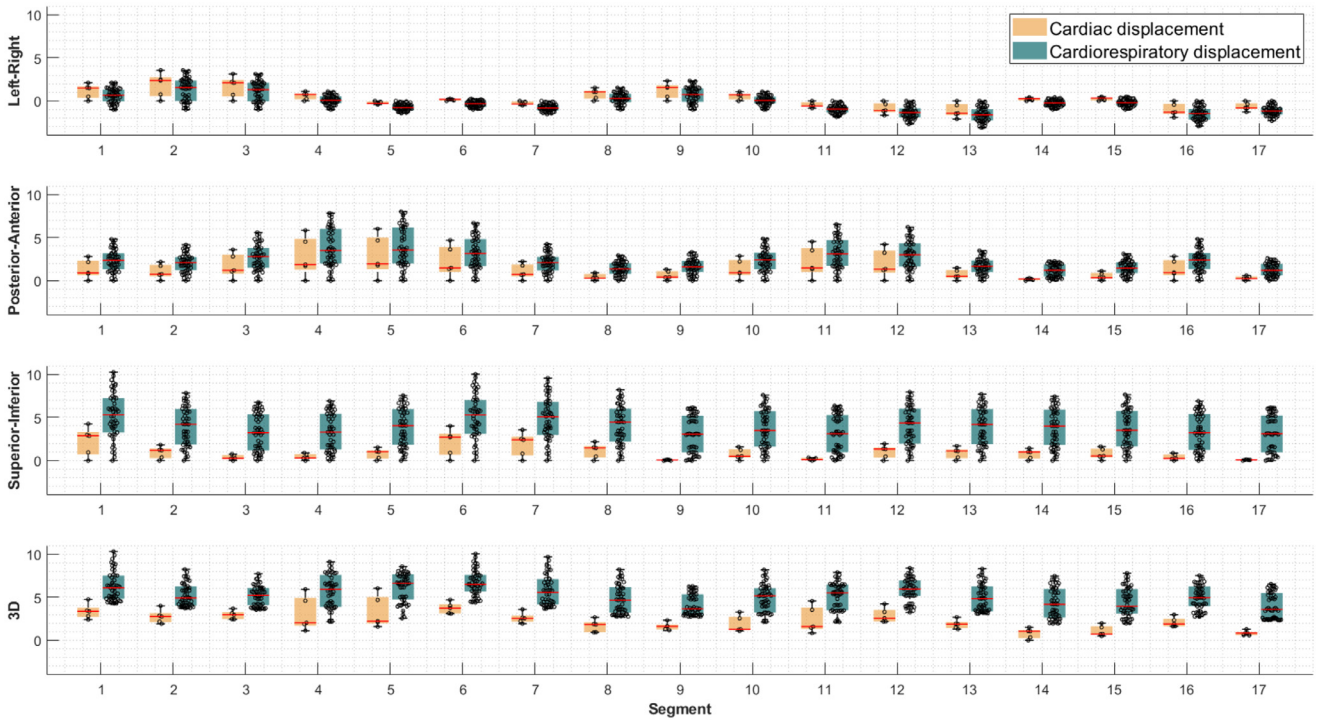

Fig. 4. Boxplots showing the centroid displacement due to cardiac (orange) and cardiorespiratory (green) motion (normalized with respect to its position in the first phase of the respective simulation) for each of the 17 segments in the left-right, posterior-anterior, and superior-inferior directions, as well as the 3D vector displacement. Displacements due to cardiac motion are taken from the inspiration breath-hold (bh) simulation and consist of 5 phases. Displacements due to cardiorespiratory motion are taken from the free-breathing (fb) simulation, which contains 50 phases. *Abbreviation*: 3D = 3-dimensional.

respiratory motion (ie, coverage for $E_{bh} < E_{fb\text{-}gat} < E_{fb\text{-}red} < E_{fb}$) for both envelopes with and without margins, whereas spillage (after adding the margin) decreased. Average coverage of target volumes without margin ranged between 67.7% and 74.8%. Although adding the 3 mm margin around the diastolic envelopes increased the average coverage to 93.5% to 95.3%, these margins also resulted in an increase of geometric spillage to 39.6% to 44.7%. In general, coverage and spillage were lower for the segments near the free wall.

Discussion

To determine the optimal approach for STAR in individual patients with VT, the effect of cardiorespiratory motion combined with different motion management strategies must be assessed. Only a limited number of studies investigated the effect of cardiorespiratory motion on STAR.[18,20] One reason for this could be the limited number of patients who are treated per center. Multicenter databases, such as the registry of the STOPSTORM.eu consortium,[11] can help to optimize STAR by investigating and defining requirements for treatment preparation and delivery. In this study, we developed a digital phantom framework that allows simulation of patient-specific cardiac and respiratory motion for patients with VT. The framework can be used to generate a huge amount of detailed data, such as 3D CT scans at many different time points, for a wide range of different motion management scenarios. In addition, the expansion of the XCAT phantom with the AHA 17-segment model enables the implementation of patient-specific target volumes. Moreover, within the framework, cardiac contraction, respiratory motion, geometry, and anatomy, can be varied while keeping other parameters constant, something that can be challenging or even impossible in patient studies. Such individualized customization of a user-defined "ground-truth" facilitates a thorough and detailed analysis of motion and its effects on STAR accuracy. We showed a use case in which we investigated the geometric effect of cardiorespiratory motion in combination with different motion management techniques to show the possibilities of the framework. By prescribing population-averaged cardiorespiratory motion amplitudes of patients with VT, we generated 3D CT scans at 50 different time points for a free-breathing scenario. Subsequently, we used this benchmark to create 4 other scenarios that mimicked different motion management techniques.

Target volumes of the 17 segments ranged between 1.2 and 9.0 cm^3. Although these values are within the ranges of 3.5 to 109 cm^3 reported in literature,[10,19] our target volumes are on the low side of the spectrum. This can be explained by the fact that clinical STAR targets often comprise multiple (parts of) segments, whereas our targets consisted of

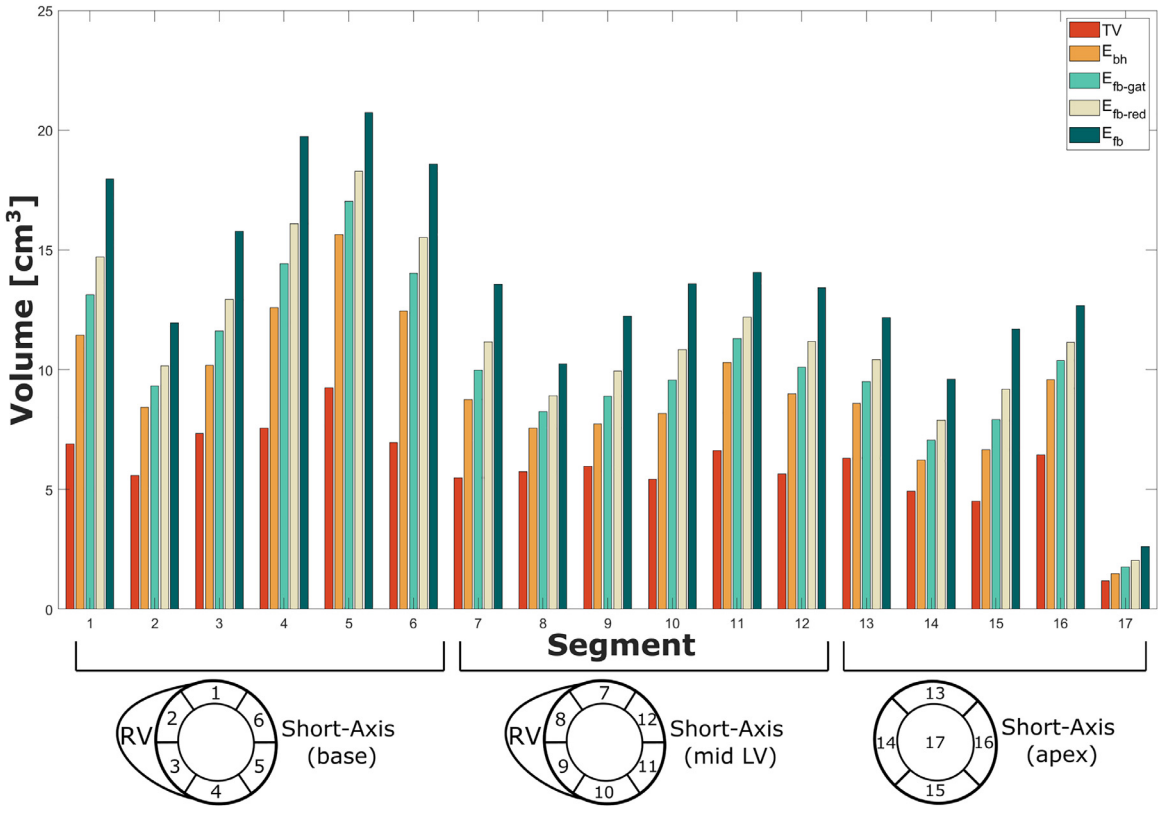

Fig. 5. Volumes of the 17 segments (TV) and the corresponding motion envelopes (E) for the 4 simulated scenarios, that is, breath-hold (bh), respiratory-gating (fb-gat), reduced free-breathing (fb-red), and free-breathing (fb). *Abbreviations*: LV = left ventricle; RV = right ventricle; TV = target volume.

single segments of the 17-segment model. This was a deliberate choice as our aim was to gain insight into the effect of motion for different regions of the heart. Nevertheless, more clinically realistic targets constructed from multiple (parts of) segments could result in more complex and different motion results compared with the ones shown here. Especially when STAR targets consist of segments that each display large cardiac motion in a different direction, for example the combination of segments 2 and 3 (both displaying larger motion in LR), with segment 4 (large motion in PA), the contribution of cardiac contraction to the total motion envelope could become somewhat larger than when the individual segments are considered. In contrast, the centroid movement of this target could be smaller than for the individual segments because the motions in opposite directions cancel each other out. Moreover, applying an isotropic margin on top of the diastolic volume of such a multisegment target could result in less spillage compared with a single segment target, because the multisegment target shows movement in more directions during cardiac contraction-relaxation and thus covers the extra volume created by the additional margin better.

Although our results cannot be translated directly to clinical target volumes, they give clinicians a better understanding of the cardiac (and respiratory) motion of the different segments. In addition, they show the effect that cardiac motion can have on the motion envelope for targets located in different regions of the heart.

Table 1 Volumes, coverage, and spillage of the envelopes constructed using only the diastolic cardiac phases (E_{x_dia}), with and without the additional 3 mm margin, for the following simulated scenarios: breath-hold/cardiac motion only (bh), respiratory-gating (fb-gat), reduced respiratory motion (fb-red), and free-breathing (fb)

		Coverage (%)		Spillage (%)	
	Volume (cm^3)	Diastolic	Diastolic + 3 mm	Diastolic	Diastolic + 3 mm
E_{bh_dia}	6.0 (1.2 9.3)	67.7 (56.0 80.7)	93.5 (80.0 100)	0 (-)	44.7 (36.9 65.9)
$E_{fb\text{-}gat\_dia}$	7.0 (1.5 10.3)	70.2 (59.8 82.6)	94.1 (82.0 100)	0 (-)	43.0 (35.5 63.7)
$E_{fb\text{-}red\_dia}$	8.0 (1.7 11.2)	72.1 (61.5 84.7)	94.6 (83.6 100)	0 (-)	41.7 (34.5 62.2)
E_{fb_dia}	9.9 (2.3 13.4)	74.8 (63.2 86.0)	95.3 (84.9 100)	0 (-)	39.6 (32.0 59.4)

The increase of the cardiac and cardiorespiratory envelope volumes with respect to the target volumes found in this study, that is, 24% to 79%, 79% to 167%, and 55% to 123% for cardiac motion only, free-breathing, and reduced free-breathing, respectively, are in agreement with ITV ranges observed in studies performed on patients with VT,[2,3,18,21-24] indicating that both cardiac and (cardio)respiratory motion of our phantom is comparable to motion in patients with VT. The effect of cardiac motion, as presented here, might especially be of importance for centers that deliver treatment using a respiratory tracking system, such as CyberKnife. Even though respiratory tracking might not require a respiratory margin, clinicians still must decide whether or not a margin is applied to cover cardiac motion. Some studies that use respiratory tracking do not consider cardiac motion.[10] However, our results show that the cardiorespiratory envelopes that only included the diastolic phase of the cardiac cycle (E_{fb_dia}), covered 63% to 86% of the cardiorespiratory motion, indicating that cardiac motion can have a major effect. Furthermore, the outcomes of this study can aid in the decision of treatment margins. Expanding the envelopes with the 3 mm margin to account for cardiac motion, an approach commonly used for treatments with robotic respiratory-tracking systems,[18,19] showed increased coverage but also resulted in spillage of 32% to 60% depending on the location of the target volume. Moreover, both our results as well as the study by Bellec et al[18] show that fixed margins on top of the diastolic target volume cannot fully correct for cardiac contraction, especially when the target is located at the free wall of the LV. Depending on the location of the target, our segment-wise results can guide clinicians in considering anisotropic instead of isotropic margins in their treatment plan, which might result in a reduction of treated healthy tissue. Moreover, clinicians can compare the (cardiac) and respiratory motion of our simulations with the motion of their clinical patient to obtain a crude estimation of the possible reduction in treatment volumes that could be achieved by using respiratory motion management techniques.

Based on the geometric effect that cardiac motion can have on the motion envelopes, we advise patient-specific evaluation of cardiac motion to sufficiently cover the full motion envelope of the target. In a typical clinical imaging scenario 4D respiratory-binned CT scans are often used to assess respiratory motion of targets and organs at risk but are not synchronized with the heart rate. The frequency of cardiac contraction is higher than the frequency of breathing motion, causing the heart to go through multiple contraction phases during the acquisition of each instance of the respiratory-binned CT scan. As a result, respiratory-binned 4D CT scans used to estimate ITVs in a clinical setting will contain a blurred representation of the heart cycle and thus captures (some) cardiac motion.[20] There is still an ongoing debate about whether a respiratory 4D CT scan can capture the cardiac motion. If the cardiac motion captured with a 4D CT covers the cardiac motion of the heart sufficiently, cardiac-binned scans would no longer be required for patients treated with free-breathing, reducing both cost and patient burden. The XCAT phantom allows the creation of CT scans at specified points in time. However, the phantom creates instantaneous snapshots of the motion instead of blurred CT scans. Although it is possible to create blurred CT scans by averaging 3D CT scans obtained from different timepoints, matching the actual 4D data acquisition of the various CT scanners that are used in the clinical setting is difficult. Therefore, studies with both physical phantom and real patients should be performed to investigate the capability of respiratory 4D CT scans to capture cardiac motion.

However, full geometric coverage during all the phases may not be required to achieve adequate dosimetric coverage. Dosimetric coverage depends, among others, on the amount of time the target is in a certain position, which will change with varying heart rates. Therefore, a full dosimetric analysis is warranted to assess the level of dosimetric coverage for different cardiac and respiratory motion patterns and target locations in combination with different motion management scenarios and treatment techniques.

In this study, we simulated an inspiration breath-hold scenario to estimate the cardiac motion envelope, but we did not simulate an expiration breath-hold scenario. Although no large differences in the cardiac motion envelopes obtained during an inspiration or expiration breath-hold scenario are expected, there will most likely be differences in the outcomes of a dosimetric analysis. During inspiration, the heart moves farther away from other structures, such as the stomach and chest wall, which can result in a lower dose to the organs at risk.[17] However, although inspiration breath-holds might be more comfortable for the patient, they can lead to larger intra-breath-hold variations in organ position of the heart and other organs due to relaxing of respiratory muscles compared with expiration breath-hold.[25-28]

Applying respiratory motion management, that is, breath-hold and respiratory-gating, in our simulations showed a decrease in the cardiorespiratory motion envelope volumes. However, the possible gain from motion management techniques depends on the location of the target and the amount of motion within a patient. In addition, gains might even be smaller due to physiological variations. For example, variations in the level of breath-hold during repeated breath-holds have been shown.[25] Moreover, the target may still move due to the aforementioned drifting of the diaphragm.[25,26] Unfortunately, many patients eligible for STAR are clinically not stable enough to tolerate breathing restrictions.[20] Influencing cardiac motion is usually not possible due to ethical and clinical reasons. New techniques that aim to deliver radiation only in certain phases of the cardiac cycle are being developed.[29] In addition, also the combination of cardiac gating with real-time tracking of respiratory motion is being investigated.[30] However, these techniques are still at an early stage and not clinically available yet. Nevertheless, cardiac-gated imaging modalities can be used to assess cardiac motion to incorporate cardiac motion during treatment planning.

The XCAT phantom is based on the anatomy and physiology of a healthy population which differs from the VT population. Although we did not alter the anatomy of the heart (eg, no dilatation of the heart was simulated) or the heart rate, we did simulate cardiac contraction and cardiorespiratory motion specifically for patients with VT. The fact that we did not alter the heart rate, however, does not influence the results of our use case because cardiac motion was only simulated to obtain the complete cardiac motion envelope. The simulated motion of a patient with VT was implemented by reducing cardiac contraction, that is, the ejection fraction, and respiratory motion of the phantom based on population data.[10] However, the extent of cardiorespiratory motion is very patient-specific and can, therefore, vary significantly between patients. Moreover, patients might have heart defects (eg, cardiac hypertrophy) causing reduced motion/contraction in specific regions of the heart. Such regional characteristics were not incorporated in the current version of the framework. Because of large variations between patients, it is almost impossible to obtain an overview of the effect of motion that is applicable to the complete VT patient population without simulating every patient. Although in theory, this can be done by changing the framework's parameters to patient-specific values, it will be a tremendous amount of work. Therefore, investigations such as the one presented in this paper together with the study of Bellec et al[18] and Harms et al[20] are essential to comprehensively understand all the motion patterns and implications for treatment.

Conclusion

We successfully developed a framework that can simulate realistic cardiac and respiratory motion in combination with various motion management strategies in the context of STAR. As an example, the framework was used to assess the geometric extent of cardiorespiratory motion of the 17 segments during 4 breathing scenarios. Our results show that if no motion management strategies are used, cardiac and respiratory motion significantly affect the motion envelope. Therefore, we advocate patient-specific assessment of both cardiac and respiratory motion during treatment planning (and delivery) to achieve optimal STAR. In future research, the developed framework can also be used to analyze radiation therapy dose distributions for different treatment and motion management strategies to perform a full dosimetric analysis.

References

1. Cuculich PS, Schill MR, Kashani R, et al. Noninvasive cardiac radiation for ablation of ventricular tachycardia. *N Engl J Med* 2017;377:2325-2336.
2. Robinson CG, Samson PP, Moore KMS, et al. Phase I/II trial of electrophysiology-guided noninvasive cardiac radioablation for ventricular tachycardia. *Circulation* 2019;139:313-321.
3. Mayinger M, Kovacs B, Tanadini-Lang S, et al. First magnetic resonance imaging-guided cardiac radioablation of sustained ventricular tachycardia. *Radiother Oncol* 2020;152:203-207.
4. van der Ree MH, Dieleman EMT, Visser J, et al. Direct clinical effects of cardiac radioablation in the treatment of a patient with therapy-refractory ventricular tachycardia storm. *Adv Radiat Oncol* 2022;7 100992.
5. Miszczyk M, Jadczyk T, Gołba K, et al. Clinical Evidence behind Stereotactic Radiotherapy for the Treatment of Ventricular Tachycardia (STAR)—A comprehensive review. *J Clin Med* 2021;10:1238.
6. Cerqueira MD, Weissman NJ, Dilsizian V, et al. Standardized myocardial sementation and nomenclature for tomographic imaging of the heart: A Statement for Healthcare Professionals from the Cardiac Imaging Committee of the Council on Clinical Cardiology of the American Heart Association. *Circulation* 2002;105:539-542.
7. Brownstein J, Afzal M, Okabe T, et al. Method and atlas to enable targeting for cardiac radioablation employing the American Heart Association segmented model. *Int J Radiat Oncol Biol Phys* 2021;111:178-185.
8. Mayinger M, Boda-Heggemann J, Mehrhof F, et al. Quality assurance process within the RAdiosurgery for VENtricular TAchycardia (RAVENTA) trial for the fusion of electroanatomical mapping and radiotherapy planning imaging data in cardiac radioablation. *Phys Imaging Radiat Oncol* 2023;25 100406.
9. van der Ree MH, Visser J, Planken RN, et al. Standardizing the cardiac radioablation targeting workflow: Enabling semi-automated angulation and segmentation of the heart according to the American Heart Association segmented model. *Adv Radiat Oncol* 2022;7 100928.
10. Stevens RRF, Hazelaar C, Fast MF, Mandija S, Grehn M, Cvek J, et al. STereotactic Arrhythmia Radioablation (STAR): Assessment of cardiac and respiratory heart motion in ventricular tachycardia patients - A STOPSTORM.eu consortium review. *Radiother Oncol* 2023;109844.
11. Grehn M, Mandija S, Miszczyk M, et al. STereotactic Arrhythmia Radioablation (STAR): The Standardized Treatment and Outcome Platform for Stereotactic Therapy Of Re-entrant tachycardia by a Multidisciplinary consortium (STOPSTORM.eu) and review of current patterns of STAR practice in Europe. *Europace* 2023;25:1284-1295.
12. Segars WP, Mahesh M, Beck TJ, Frey EC, Tsui BMW. Realistic CT simulation using the 4D XCAT phantom. *Med Phys* 2008;35:3800-3808.
13. Lowther N, Ipsen S, Marsh S, Blanck O, Keall P. Investigation of the XCAT phantom as a validation tool in cardiac MRI tracking algorithms. *Phys Medica* 2018;45:198-204.
14. Hindley N, Lydiard S, Shieh C-C, Keall P. Proof-of-concept for x-ray based real-time image guidance during cardiac radioablation. *Phys Med Biol* 2021;66 175010.
15. Segars WP, Sturgeon G, Mendonca S, Grimes J, Tsui BMW. 4D XCAT phantom for multimodality imaging research. *Med Phys* 2010;37:4902-4915.
16. Knybel L, Cvek J, Neuwirth R, et al. Real-time measurement of ICD lead motion during stereotactic body radiotherapy of ventricular tachycardia. *Reports Pract Oncol Radiother* 2021;26:128-137.
17. Cha M, Cuculich PS, Robinson CG, Chang JH. Tailored stereotactic radiotherapy technique using deep inspiration breath-hold to reduce stomach dose for cardiac radioablation. *Radiat Oncol J* 2021;39:167-173.
18. Bellec J, Rigal L, Hervouin A, et al. Cardiac radioablation for ventricular tachycardia: Which approach for incorporating cardiorespiratory motions into the planning target volume? *Phys Medica* 2022;95:16-24.
19. Lydiard PGDip S, Blanck O, Hugo G, O'Brien R, Keall P. A review of cardiac radioablation (CR) for arrhythmias: Procedures, technology, and future opportunities. *Int J Radiat Oncol* 2021;109:783-800.
20. Harms J, Schreibmann E, Mccall NS, Lloyd MS, Higgins KA, Castillo R. Cardiac motion and its dosimetric impact during radioablation for refractory ventricular tachycardia. *J Appl Clin Med Phys* 2023;21:1-9.

21. Widesott L, Dionisi F, Fracchiolla F, et al. Proton or photon radiosurgery for cardiac ablation of ventricular tachycardia? Breath and ECG gated robust optimization. *Phys Medica* 2020;78:15-31.
22. Carbucicchio C, Andreini D, Piperno G, et al. Stereotactic radioablation for the treatment of ventricular tachycardia: Preliminary data and insights from the STRA-MI-VT phase Ib/II study. *J Interv Card Electrophysiol* 2021;62:427-439.
23. Levis M, Dusi V, Magnano M, et al. A case report of long-term successful stereotactic arrhythmia radioablation in a cardiac contractility modulation device carrier with giant left atrium, including a detailed dosimetric analysis. *Front Cardiovasc Med* 2022;9 934686.
24. Knutson NC, Samson PP, Hugo GD, et al. Radiation therapy workflow and dosimetric analysis from a phase 1/2 trial of noninvasive cardiac radioablation for ventricular tachycardia. *Radiat Oncol Biol* 2019;104:1114-1123.
25. McLeish K, Hill DLG, Atkinson D, Blackall JM, Razavi R. A study of the motion and deformation of the heart due to respiration. *IEEE Trans Med Imaging* 2002;21:1142-1150.
26. Holland AE, Goldfarb JW, Edelman RR. Diaphragmatic and cardiac motion during suspended breathing: Preliminary experience and implications for breath-hold MR imaging. *Radiology* 1998;209:483-489.
27. Plathow C, Ley S, Zaporozhan J, et al. Assessment of reproducibility and stability of different breath-hold maneuvres by dynamic MRI: Comparison between healthy adults and patients with pulmonary hypertension. *Eur Radiol* 2006;16:173-179.
28. Scott AD, Keegan J, Firmin DN. Motion in cardiovascular MR imaging. *Radiology* 2009;250:331-351.
29. Poon J, Kohli K, Deyell MW, et al. Technical Note: Cardiac synchronized volumetric modulated arc therapy for stereotactic arrhythmia radioablation: Proof of principle. *Med Phys* 2020;47:3567-3572.
30. Akdag O, Borman PTS, Woodhead P, et al. First experimental exploration of real-time cardiorespiratory motion management for future stereotactic arrhythmia radioablation treatments on the MR-linac. *Phys Med Biol* 2022;67 065003.